



ÉCOLE POLYTECHNIQUE FÉDÉRALE DE LAUSANNE

CH-420. UNDERSTANDING ADVANCED MOLECULAR SIMULATION

SPRING 2022

Exercises block 3: MD and MC in various ensembles

BRUNO RODRIGUEZ CARRILLO

SCIPER 326180

PROFESSOR:
BEREND SMIT

MAY 31TH, 2022

1 Barrier crossing

We are given the potential defined in

$$U(x) = \begin{cases} \epsilon Bx^2 & x < 0 \\ \epsilon(1 - \cos(2\pi x)) & 0 \leq x \leq 1 \\ \epsilon B(x-1)^2 & x > 1 \end{cases} \quad (1)$$

1. To derive an expression for B we recall that the potential $U(x)$ and its first and second derivatives should be continuous at $x = 0$ and $x = 1$. Then we have

$$\frac{\partial U(x)}{\partial x} = \begin{cases} 2\epsilon Bx & x < 0 \\ 2\pi\epsilon \sin(2\pi x) & 0 \leq x \leq 1 \\ 2\epsilon B(x-1) & x > 1 \end{cases} \quad (2)$$

$$\frac{\partial^2 U(x)}{\partial^2 x} = \begin{cases} 2\epsilon B & x < 0 \\ 4\pi^2\epsilon \cos(2\pi x) & 0 \leq x \leq 1 \\ 2\epsilon B & x > 1 \end{cases} \quad (3)$$

Then for the second derivative (3) to be continuous at $x = 0$ and $x = 1$, we have

$$2\epsilon B = 4\pi^2\epsilon \rightarrow B = 2\pi^2$$

And we have obtain figure (1) when we vary ϵ . As observed, the potential function and its first and second derivatives are continuous by using the value of B previously computed. Moreover, changing the value of ϵ implies modifying the position of the barrier, point $x = 0.50$. That is, the larger ϵ , the higher the barrier, and thus, the more energy it takes for a particle to go from one minimum to the other.

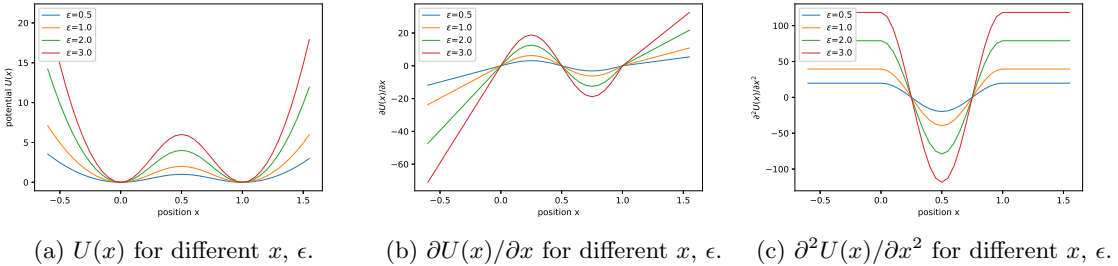


Figure 1: $U(x)$, $\partial U(x)/\partial x$ and $\partial^2 U(x)/\partial x^2$ for different values of ϵ .

2. In the following figures we plot how the phase space trajectories look like for different methods. It is important to mention that we tried each of these methods for three different values of temperature $T \in \{0.10, 0.50, 2\}$ and for distinct method-dependent parameters as indicated in each figure. Moreover, explanations on each will be given in next points.

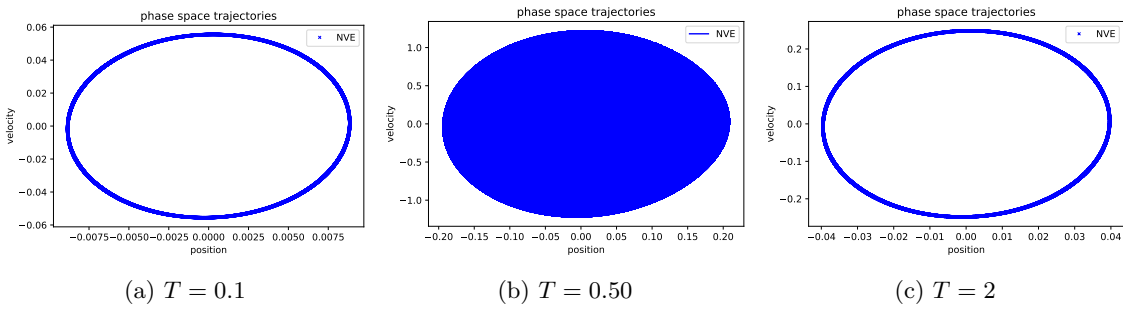


Figure 2: Phase space for the NVE ensemble.

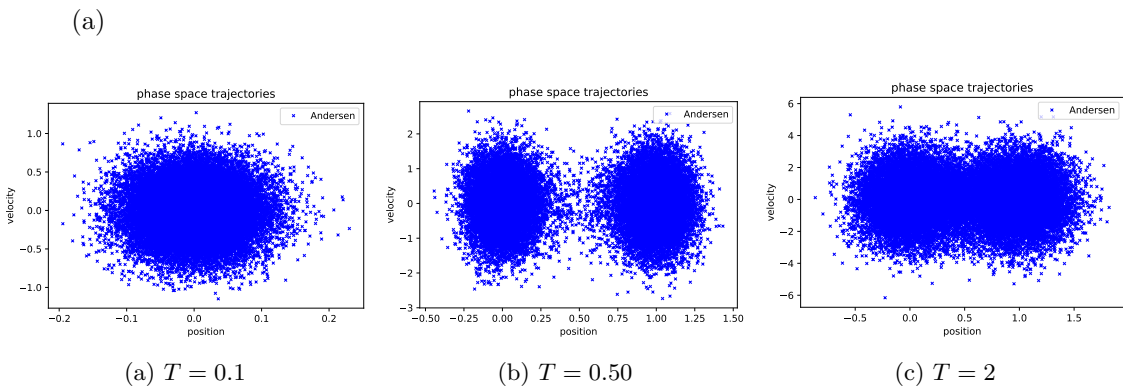


Figure 3: Phase space for the Andersen thermostats.

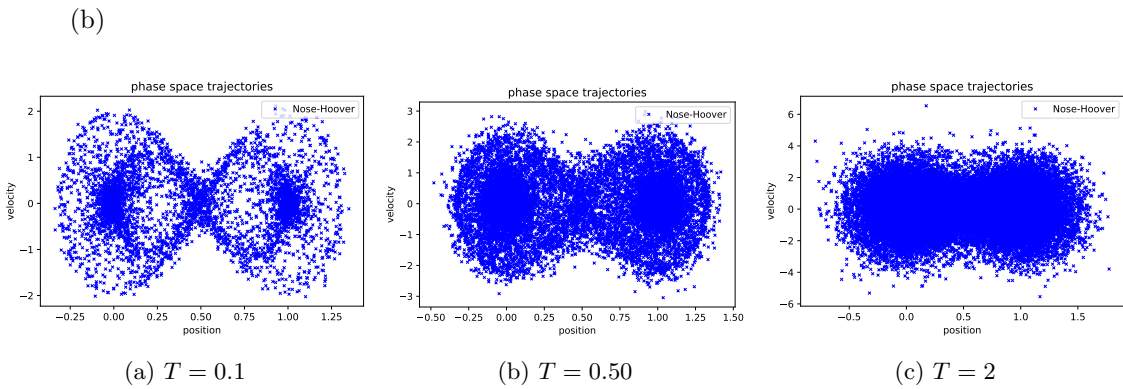


Figure 4: Phase space for the Nose-Hoover chain, one chain.

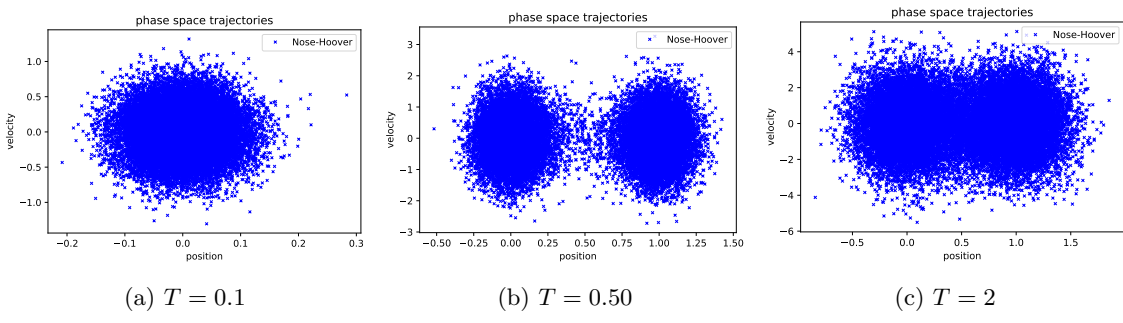


Figure 5: Phase space for the Nose-Hoover chain, five chains.

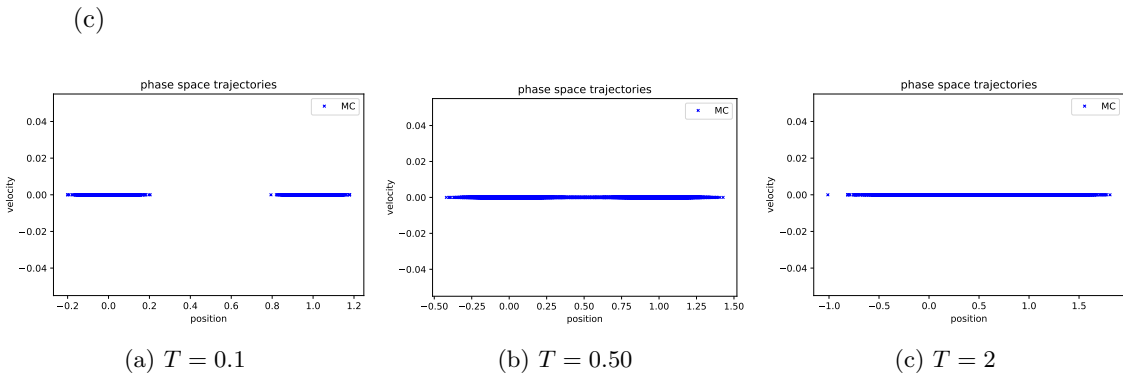


Figure 6: Phase space for Monte Carlo.

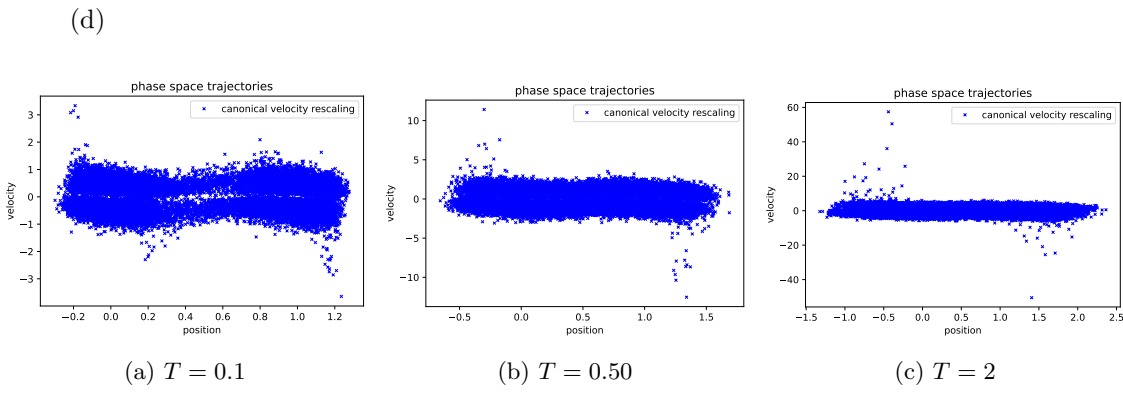


Figure 7: Phase space for Berendsen with stochastic term.

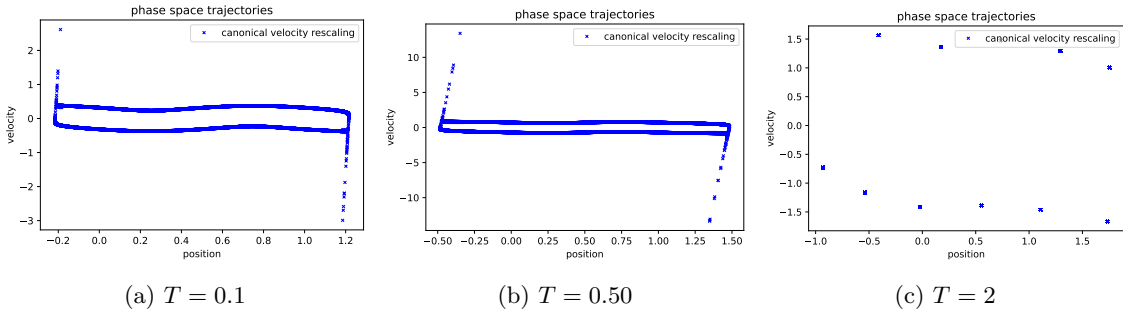


Figure 8: Phase space for Berendsen without stochastic term.

(e)

3. Apart from all previous figures, we will be using figures X a and YY to analyze figures shown in point 2.

(a) From figure 6- a), we observe that the particle is moving around the two dwells of our potential function. However, we should notice that the phase space in our MC simulation looks like a couple of aligned straight lines since in Monte Carlo we do not sample velocities. That is, in this type of simulations, we are actually interested in computing the particle's position only since it is position what we need to compute the average ensemble of a given property of interest; this is what an MC simulation is run for. In addition, and it is relevant to realize, we are obtaining samples in both dwells but we do not see any sample between the two dwells.

On the other hand, in figure 6- b) and c), we do see that the particle crosses the potential barrier. Again, we see a line since we are just sampling position and not velocities.

(b) Regarding figure 2, we observe that the particle moves around a circle. The reason behind this behaviour is the fact that the particle follows a trajectory that is the one corresponding to a fixed energy level, see figure (9), we should keep in mind that our potential is symmetric.

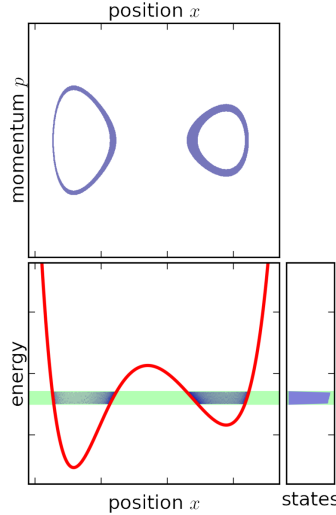


Figure 9: Example of an NVE ensemble phase space.

Figure 9 is illustrative for an NVE ensemble since we observe that for an interval of energy, the particle's position is allowed moving around trajectories within this energy interval.

Thus, in any plot shown in figure 2, we clearly observe that the particle is confined in one of the potential dwells and it is incapable of crossing the potential barrier. Moreover, we state that the particle does not explores the whole sample space but just those states allowed by its energy level.

- (c) In case of the Nosé-Hoover chain method, figures 4 and 5, we notice that for one chain the phase space is sampled more uniformly from $T = 0.1$ and $T = 0.50$ than for five chains. This may occur since in the latter, we coupled five thermostats, which leads to harder "linking" of their dynamics. It is quite interesting to observe that we require one chain to obtain the canonical distribution at any of the shown temperatures. But at $T = 2$, the phase space sampled by five chains is evidently larger than its counterpart for one chain.

For the Andersen thermostat, figure 3, the frequency of collision is 10 and we clearly observe that for low temperatures, we do not sample the phase space properly, i.e. the particle is confined inside a dwell of the potential function and then, it does not cross the energy barrier. However, as temperature increases, the phase space is sampled better.

In either of these methods, we know that at high temperatures, the particle possesses more energy and it is then when it capable of moving throughout the phase space, as expected in theory.

Thus, we state that for $T = 0.50$ the Andersen and Nosé-Hoover methods lead to the canonical distribution.

4. To investigate at which temperature the particle is able to cross the energy barrier, we first recall that in the NVE ensemble it is not possible to sample the whole phase space since our system is restricted to follow trajectories with a fixed value of energy.

On the other hand, the particle is able to cross the energy barrier when there exist a trajectory connecting both dwells of the potential function; that is, we should observe a trajectory joining both dwells. In our case, we thus say that the particle crosses the energy barrier when we obtain points in both dwells and between them. Consequently, from figures shown in point 3, we could say that for temperatures $T \geq 0.50$, the particle is able to cross the energy barrier.

5. First, we recall that the Berendsen thermostat suppresses fluctuations of the kinetic energy of the system and therefore cannot produce trajectories consistent with the canonical ensemble. When we remove the stochastic term from the re-scaling factor, we observe that the particle is not able to visit all states in the phase space. One reason why this happens is due to the fact that the scaling factor with no stochastic term is actually just a constant that multiplies the velocity at each time step. As a result, we sample those states corresponding to a given position and velocity.

Besides, in figures 8, we can notice that for any of the three temperatures shown, the particle seems to be moving around the potential's external boundary, but this happens in fixed trajectories. In a) and b), the particle follows a trajectory that seems to be near the minima of the potential. On the contrary, in c), the particle's trajectory, in fact, seems to diverge from any of the minima but again it follows a specific path. This case is interesting since the particle looks like moving away from the minimum points. But it is also important to realize that the particle actually crosses the energy barrier for the three temperatures shown.

When we have a look at 7, we observe a similar pattern, but the main difference now is that the particle explores other regions of the phase space. This happens because we include the stochastic term and then the particle has more freedom to move around in the phase space. However, there are missing points that the particle does not visit; it looks like there are configurations that the particle cannot access to and thus the sampling is restricted to a subset of actual accessible states. This is the reason why the phase space looks a bit flatten when compared to the Andersen's or Nose-Hoover's.

6. We now change our potential function to

$$U = \epsilon(1 - \cos(2\pi x)) \text{ and } F = 2\pi\epsilon \sin(2\pi x), -\infty < x < \infty, \quad (4)$$

which is implemented in the code *force.c*.

Let us state in words that diffusion consists of a substance moving from an area of high concentration to an area of low concentration until the concentration is equal across a given volume. Then, diffusion requires motion to happen. Consequently, it is not possible to compute the diffusivity at low temperatures since the lower the temperature is, the less kinetic energy a system's particles have. Thus, higher temperatures increase the energy and therefore the movement of the molecules, increasing the rate of diffusion. Lower temperatures decrease the energy of the molecules, thus decreasing the rate of diffusion.

It can be shown that the Andersen thermostat correctly generates the canonical ensemble and therefore can be used to calculate equilibrium properties. However, since it uses fictitious dynamics, it is not intuitively clear whether the Andersen thermostat can be used to calculate dynamic quantities such as the diffusion coefficient. [3]

As shown in [3] for a particular system, the diffusion coefficient computed using molecular dynamics with the Andersen thermostat depends sensitively on the value of the collision rate

in the thermostat. This is a consequence of the fact that there are no intrinsic time scales of mixing in such systems, and if the underlying system does have intrinsic diffusion, then the diffusion coefficient computed using the Andersen thermostat does converge to the correct value in the limit of zero collision frequency in the thermostat.

In general, there are two competing time scales: One is set by the maximal Lyapunov exponent of the chaotic Hamiltonian dynamics and gives rise to diffusion. The other is set by the collision frequency of the thermostat. In the limit of vanishing collision frequency, the system should spend most of its time doing “deterministic diffusion.” Therefore the diffusion constant calculated using the Andersen thermostat should not be too different from the deterministic diffusion constant. [3]

We then simulate and compute the diffusion coefficient for the potential function (4) for various temperatures. The results are shown in figure 10 and table 1.

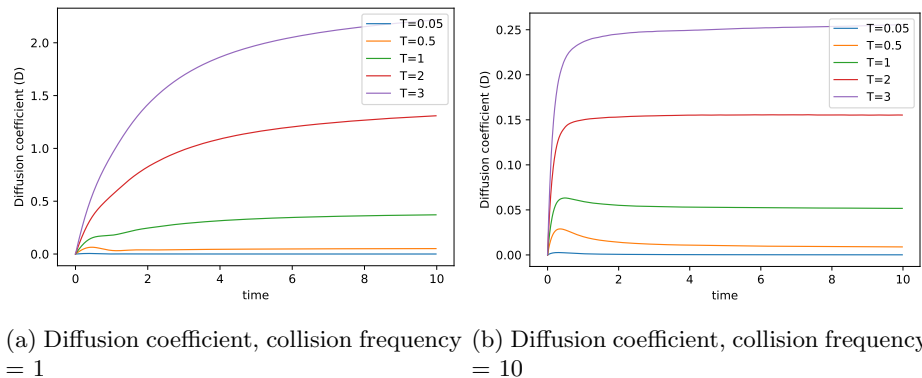


Figure 10: Diffusion coefficient for different frequencies of collision.

T	0.05	0.5	1	2	3
D , frequency = 10	0.000131	0.008907	0.051682	0.155301	0.255736
D , frequency = 1	0.000132	0.051383	0.371237	1.308827	2.216673

Table 1: Values of the D .

It should be noticed that we use the MSD method to compute the value of D at each T . as can be observed, the values of D change significantly when modifying the frequency of collision in the Andersen thermostat.

2 MC in the NPT ensemble

1. We refer to the formal definition of hard spheres: hard spheres of diameter σ are particles with the following pairwise interaction potential:

$$V(\mathbf{r}_1, \mathbf{r}_2) = \begin{cases} 0, & |\mathbf{r}_1 - \mathbf{r}_2| \geq \sigma \\ \infty, & |\mathbf{r}_1 - \mathbf{r}_2| < \sigma \end{cases}, \quad (5)$$

where \mathbf{r}_1 and \mathbf{r}_2 are the positions of two particles. From (5), it is clear that it would not be possible to compute the virial of this system since the potential is discontinuous when $|\mathbf{r}_1 - \mathbf{r}_2| < \sigma$, and as we know from previous exercises, we may compute the virial of the system by using the derivative of the the potential interaction. Due to discontinuity of V , the virial cannot be computed.

2. The code for a random walk in $\ln(V)$ and in V looks like

```
//Vnew=exp(log(Vold)+(RandomNumber()-0.5)*MaximumVolumeChange); SAMPLING ln(V)
Vnew=(Vold + (RandomNumber()-0.5)*MaximumVolumeChange); // SAMPLING V
// no overlap... use acceptance rule
if((!overlap)&&(RandomNumber()<exp(-Beta*Pressure*(Vnew-Vold)+log(Vnew/Vold)*(NumberOfParticles)))) // SAMPLING V
//if((!overlap)&&(RandomNumber()<exp(-Beta*Pressure*(Vnew-Vold)+log(Vnew/Vold)*(NumberOfParticles+1.0)))) SAMPLING ln(V)
```

Figure 11: code change for random walk in $\ln(V)$ and V .

To observe which value are required to have the same average densities, we performed a few trial simulations to tune our parameters maximum volume change ΔV_{max} and pressure P whereas our remaining parameters remained unchanged for each simulation.

Thus we found that for a pressure $P = 1$ and $\Delta V_{max} = 2.2$, the average densities $\bar{\rho}$ for each algorithm are $\bar{\rho}_V = 0.3026$ and $\bar{\rho}_{\ln(V)} = 0.3079$, respectively.

3. Firstly, we should notice that in figure 12, there are two regions where the acceptance ratios are alike: small or large change of volume. The reason why this happens is due to the fact that small changes in volume will be almost always acceptance no matter if we sample in V or $\ln(V)$. We may think of a small change of volume as our system slowly evolving or changing during our simulation, which implies taking many samples to ensure we sample the phase space as much as possible. A large change of volume is unlikely to happen since this would imply a large change of energy. Under such circumstance, many of the trial moves will be rejected, slowing our simulation down.

In figure 12, we clearly observe that the acceptance ratio of the trial moves in V are higher for $10^{-3} \leq \Delta V_{max} \leq 1$. This occurs since a change of volume in $\ln(V)$ is larger than in V , which as discussed previously, implies larger changes in energy between the current state and the trial move, and the big changes in energy are unlike to happen. However, this does not mean that sampling in $\ln(V)$ would be inefficient due to rejected moves. It is quite the opposite; when we perform our sampling in $\ln(V)$, we actually take larger steps and as long as these are not too large, we sample the configuration space more efficiently than sampling in V since we explore more regions -exploring these regions will probably imply a longer simulation for sampling in V . This follows what is presented in [1].

Consequently, we could sample in $\ln(V)$ and, as stated in [2], having a acceptance ratio of 50% will ensure a proper sampling of the configuration space.

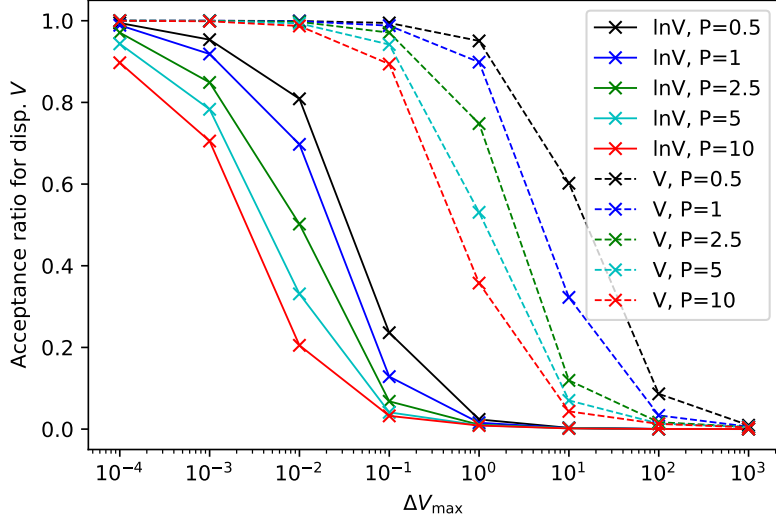


Figure 12: Acceptance probability when sampling in V and $\ln(V)$ as a function of ΔV_{max} .

3 Parallel tempering

1. To derive the ratio of acceptance probabilities, we notice that we select two different systems i and j at random such that they are consecutive states from low to high temperature; that is, $|i - j| = 1$. Then, we exchange these both by choosing $x_i(n) = x_j(o)$ and $x_j(n) = x_i(o)$, where o and n stand for old and new state, respectively.

We start by writing the detailed balanced equation (6)

$$N(i, \beta_i)N(j, \beta_j)\alpha [(i, \beta_i), (j, \beta_j) \rightarrow (j, \beta_i), (i, \beta_j)] acc [(i, \beta_i), (j, \beta_j) \rightarrow (j, \beta_i), (i, \beta_j)] = N(i, \beta_j)N(j, \beta_i)\alpha [(i, \beta_j), (j, \beta_i) \rightarrow (i, \beta_i), (j, \beta_j)] acc [(i, \beta_j), (j, \beta_i) \rightarrow (i, \beta_i), (j, \beta_j)]. \quad (6)$$

Moreover, we assume that in our Monte Carlo moves the a priori probability α to have a move is independent of the configuration; that is the probability of moving from an old position to the new position are equal. In the canonical ensemble the number of configuration in a given state n is proportional to the Boltzmann factor, i.e. $N(n) \propto \exp(-\beta U(n))$. Thus we have that the ratio of acceptance probabilities is given by after re-arranging the exponential terms:

$$\frac{acc [(i, \beta_i), (j, \beta_j) \rightarrow (j, \beta_i), (i, \beta_j)]}{acc [(i, \beta_j), (j, \beta_i) \rightarrow (i, \beta_i), (j, \beta_j)]} = \exp [(\beta_i - \beta_j)(U(x_i(o)) - U(x_j(o)))], \quad (7)$$

where we use the fact that the energies $U(j)$ and $U(i)$ correspond to the energies of system $x_j(o)$ and $x_i(o)$, respectively.

2. As observed in figure 13, the particles start diffusing at $T = 0.05$. This is observe, in the same figure, when the probability of finding a particle at any position is different from 0. We clarify that we perform an independent simulation for each value of T .

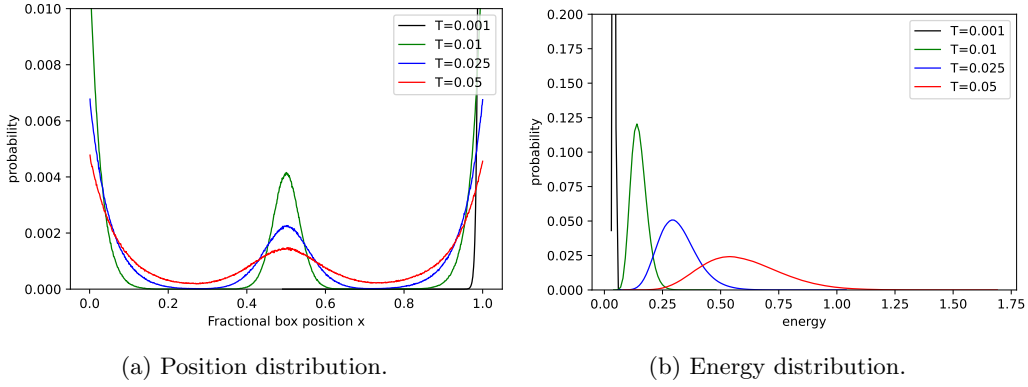


Figure 13: Position and energy distributions when no exchange moves are allowed.

3. When we allow system exchange, we observe in figure 14 that we would need 4 systems to see the particle diffusing. We simulated for $T = 0.001, 0.003, 0.015, 0.05$.

We should notice that to observe the particle diffusing the value of temperature need not be close to each other or not too far apart. By doing this, we would ensure that each of the simulated system is unlikely to be exchanged. In other words, the systems should not be too similar but not too different either.

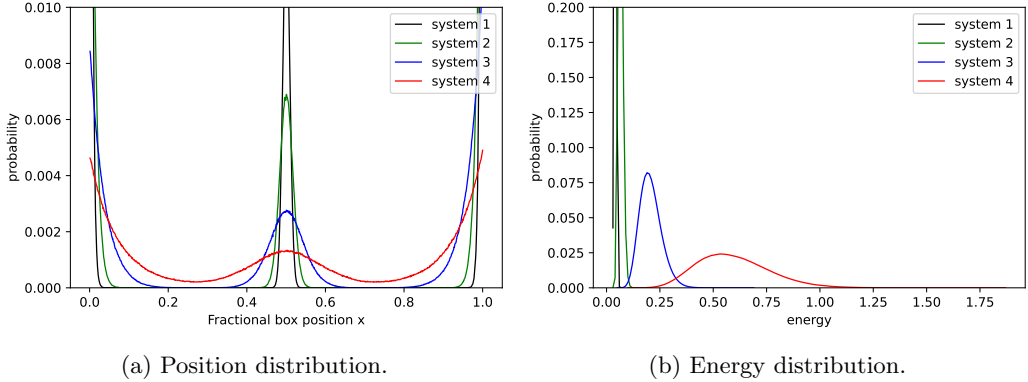


Figure 14: Position and energy distribution when no exchange moves are allowed.

the energy distributions shown in figure 13 and (14) merit some further discussion. As we know from theory, at lower temperatures, the particle has less energy. Therefore, its speed is lower and the energy distribution has a smaller range, which means that its energy distribution is expected to be skewed to the left (low energy levels). This is why these figures show a highly skewed-to-the-left energy distribution for low temperatures. As the temperature of the particle increases, the energy distribution flattens out. Because the particle has more energy at higher temperature, it moves faster. Our figures are consistent with this too.

4. In figure 15, we keep the results from system 4, previous point, and simulate again when no exchanges are allowed for $T = 0.05$ only. We clearly see that the distributions for position and energy in both cases are basically identical and the particle diffuses.

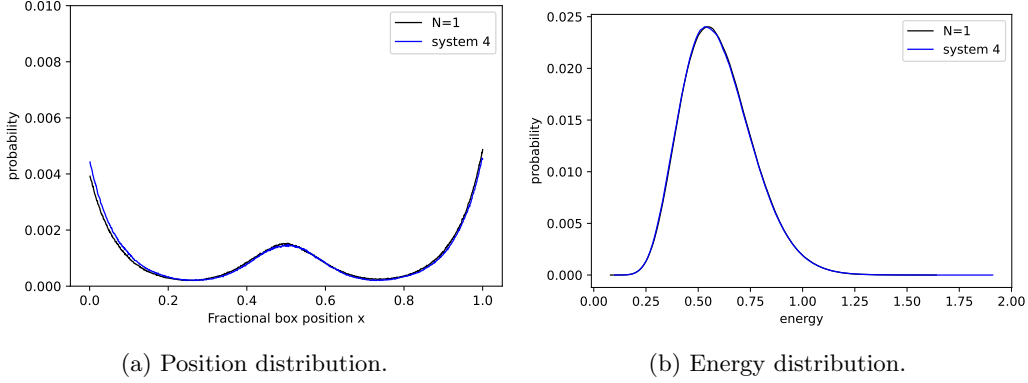


Figure 15: Position and energy distribution at $T = 0.05$.

References

- [1] Daan Frenkel and Berend Smit. *Understanding molecular simulation: from algorithms to applications*. Vol. 1. Elsevier, 2001.
- [2] Jos Thijssen. *Computational physics*. Cambridge university press, 2007.
- [3] E Weinan and Dong Li. “The Andersen thermostat in molecular dynamics”. In: *Communications on pure and applied mathematics* 61.1 (2008), pp. 96–136.